A&A 510, A79 (2010)
DOI: 10.1051/0004-6361/200911977

Astronomy & Astrophysics

Electron excitation collision strengths for transitions in K II⋆

S. S. Tayal and O. Zatsarinny

[1] Department of Physics, Clark Atlanta University, Atlanta, GA 30314, USA
[2] Department of Physics and Astronomy, Drake University, Des Moines, IA, 50311, USA
e-mail: stayal@cau.edu

Received 2 March 2009 / Accepted 30 November 2009

ABSTRACT

Aims. Oscillator strengths and electron impact excitation collision strengths for transitions between the 43 fine-structure levels of the $3p^6$, $3p^54s$, $3p^53d$, $3p^54p$, $3p^54d$ and $3p^55s$ configurations in K II are calculated. Thermally averaged collision strengths are presented as a function of electron temperature for application to astrophysical plasmas.

Methods. The B-spline Breit-Pauli R-matrix method is used to investigate the electron impact excitation of forbidden and allowed transitions in singly ionized potassium. The relativistic effects have been incorporated through mass, Darwin and spin-orbit one-body operators in the Breit-Pauli Hamiltonian in the scattering calculation, while in the calculation of oscillator strengths the one-body and two-body relativistic operators are included. Flexible non-orthogonal sets of spectroscopic and correlation radial functions are used to obtain accurate description of K II levels and to represent the scattering functions. The 43 fine-structure levels of the $3p^6$, $3p^54s$, $3p^53d$, $3p^54p$, $3p^54d$ and $3p^55s$ configurations have been considered in both the radiative and scattering calculations.

Results. The present cross sections for the excitation of the lowest 4s and 3d states show reasonable agreement with the previous R-matrix calculations. The calculated excitation energies are in excellent agreement with experiment and represents an improvement over the previous calculation. The oscillator strengths for transitions from the ground state normally compare very well with previous calculations, but for transitions from the metastable state a large discrepancy was found with other calculations. The effective collision strengths are obtained by integrating total resonant and non-resonant collision strengths over a Maxwellian distribution of electron energies and these are presented over a wide temperature range.

Key words. atomic data – atomic processes – line: formation

1. Introduction

Oscillator strengths and electron-ion collision processes play an important role in the understanding of the physical processes and conditions in various types of plasmas. The singly ionized potassium has been detected in Io's atmosphere (Kuppers & Schneider 2000; Fegley & Zolotov 2000). Accurate oscillator strengths and electron excitation collision strengths for transitions in K II are important for the diagnostics of Io's atmosphere and plasma torus. The prominent emission lines in the spectrum of K II arise due to the $3p^6\ ^1S_0$–$3p^54s\ ^1P^o_1$, $3p^6\ ^1S_0$–$3p^54s\ ^3P^o_1$, $3p^6\ ^1S_0$–$3p^53d\ ^1P^o_1$, $3p^6\ ^1S_0$–$3p^53d\ ^1P^o_1$ and $3p^6\ ^1S_0$–$3p^53d\ ^3P^o_1$ fine-structure transitions. These lines occur in the extreme ultraviolet (EUV) region of the spectrum and should be observable by the EUV spectrometers on board space missions.

The excitation energy levels, oscillator strengths and electron excitation cross sections for transitions in K II have been studied both theoretically and experimentally. The most recent measured excitation levels of K II have been reported by Peterson et al. (2007). Tayal & Zatsarinny (2008) calculated cross sections for excitation of the $3p^53d$, $3p^54s$, $3p^54p$, $3p^55s$ and $3p^54d$ levels from the ground $3p^6\ ^1S_0$ level using the B-spline Breit-Pauli R-matrix (BSR) computer code (Zatsarinny 2006). The accurate description of K II target wave functions was obtained by taking a proper account of the strong term dependence of the valence orbitals and an adequate treatment of large correlation corrections and relaxation effects. Berrington et al. (2006) reported an intermediate-coupling frame transformation R-matrix (icfRM) calculation for the excitation of the $3p^53d$, $3p^54s$, $3p^54p$, $3p^55s$ and $3p^54d$ levels. The experimental study of excitation cross sections of K II were reported by Zapesochny et al. (1986) using the crossed-beams technique. Both the BSR and icfRM calculations predicted large discrepancies with experimental cross sections in magnitude as well as in near threshold resonance structure. The overall agreement between the two calculations was found to be reasonable for the excitation of the $3p^54s$ and $3p^53d$ states, but large discrepancies up to a factor of 3 were noted for the excitation to the higher-lying $3p^54p$, $3p^55s$ and $3p^54d$ states. The discrepancies between the BSR and icfRM calculations were mainly attributed to the differences in the description of target states and in the scattering models. The term dependence effects have been found to be most important for the $3p^53d\ ^1P^o_1$ and $3p^54p\ ^1S_0$ states. There are large correlation corrections for the $3p^53d\ ^3P^o$ state due to the strong penetration of the 3d electron in the core. We have extended B-spline Breit-Pauli R-matrix calculation of Tayal & Zatsarinny (2008) to calculate effective collision strengths for all allowed and forbidden transitions among the 43 fine-structure levels. We have also calculated oscillator strengths and transition probabilities for the allowed and intercombination lines among these levels.

2. Excitation energies, oscillator strengths and lifetimes

The K II wave functions exhibit large correlation corrections due to the core-valence interaction and strong term dependence of

⋆ Tables 2–4 are only available in electronic form at the CDS via anonymous ftp to cdsarc.u-strasbg.fr (130.79.128.5) or via http://cdsweb.u-strasbg.fr/cgi-bin/qcat?J/A+A/510/A79

the one-electron valence orbitals in the $3p^5nl$ configurations. In addition, there is a strong interaction between the $3p^5(n+1)s$ and $3p^5nd$ Rydberg series together with strong spin-orbit mixing of different terms. The K II target state wave functions have been constructed with non-orthogonal orbitals that are optimized for each atomic state separately to account for the term dependence. Our calculations are performed using the multiconfiguration Hartree-Fock (MCHF) method (Froese Fischer 1991; Zatsarinny & Froese Fischer 2000). The 43 K II bound levels of the $3p^6$, $3p^53d$, $3p^54s$, $3p^54p$, $3p^55s$ and $3p^54d$ configurations have been considered in our work. These states show different correlation patterns. We first generated the spectroscopic 1s, 2s, 2p, 3s and 3p core orbitals from a Hartree-Fock (HF) calculation for the K^{2+} $3s^23p^5$ ground state. The term dependent excited orbitals 4s, 3d, 4p, 5s and 4d were then generated in separate HF calculations for each $3p^5nl$ $^{1,3}L$ state. The HF $3p^5nl$ wave functions were improved by the correlation functions ($\overline{8l}$, $\overline{9l}$; $l = 0-4$) with a 3s, 3p-excited core. The correlation orbitals $\overline{nl}$ were optimized for each term separately.

The spectroscopic and correlation functions are used to construct configuration-interaction (CI) expansions for different atomic states by allowing one-electron and two-electron excitations from all the basic configurations mentioned above. In the construction of CI expansions for fine-structure levels with various J and π we used configurations generated in this excitation scheme for the LS states and with insignificant configurations with coefficients less than 0.001 omitted from the expansions. The final CI expansions for the even and odd parity fine-structure J levels contain from 26 to 167 configurations. We used 149 different non-orthogonal orbitals in our calculations. The excitation energies of fine-structure levels relative to the ground level are reproduced in Table 1 from the work of Tayal & Zatsarinny (2008). Our results have been compared with measured values from Peterson et al. (2007) and the NIST compilation (http://physics.nist.gov). The agreement between our calculation and the experiment is excellent for the lower-lying levels of the $3s^54s$ and $3p^53d$ configurations and is very good for the higher levels. The accuracy of the higher-lying levels is slightly less than that for the lower-lying levels. The term dependence effects are most strong for the $3p^53d$ $^1P^o_1$ and $3p^54p$ $^1S_0$ states. The present calculation represents an improvement over the calculation of Berrington et al. (2006) who used a set of the same orthogonal one-electron orbitals to represent all target states. We believe that our wave functions correctly represent the main correlation corrections, the interactions between different Rydberg series and term dependence effects. The theoretical lifetimes calculated in length form for various fine-structure levels are also displayed in last column of Table 1. We are not aware of any other theoretical or experimental lifetimes for the fine-structure levels of K II.

The oscillator strengths for the dipole-allowed transitions from the ground $3p^6$ $^1S_0$ and first metastable $3p^54s$ $^3P^o_2$ levels were compared by Tayal & Zatsarinny (2008) with the CI calculation of Berrington et al. (2006), the relativistic configuration-interaction (RCI) calculation of Beck (2002), the results calculated by Smirnov & Shapochkin (1979) from lifetime measurements and the measured values of Henderson et al. (1997). A rather reasonable agreement between different calculations was noted for transitions from the ground level except for the $3p^6$ $^1S_0$–$3p^54s$ $^3P^o_1$ and $3p^53d$ $^1P^o_1$ transitions where noticeable discrepancies were noted. For oscillator strengths from the first metastable level, the CI calculations of Tayal & Zatsarinny (2008) and Berrington et al. (2006) showed good agreement with each other, but large discrepancy was noted with the calculation of Smirnov & Shapochkin (1979). In the present paper, we present oscillator strengths and transition probabilities for all allowed and intercombination lines between the 43 fine-structure levels in Table 2. The initial and final levels of a transition are given in Cols. 1 and 2 and in Col. 3 we have listed the corresponding indices of these levels from Table 1. The relativistic effects were included through the spin-orbit, spin-other-orbit, spin-spin, mass and Darwin Breit-Pauli operators. The values of oscillator strengths for intercombination lines are usually much smaller than those for the allowed transitions. The intercombination lines are induced by the spin-orbit interaction by causing mixing between different LS symmetries with the same set of quantum numbers J and π. The agreement between the length and velocity forms of oscillator strengths may to some extent indicate the accuracy of wave functions and convergence of CI expansions. However, it is not a sufficient condition for the accuracy of results. The convergence of results is an important

Table 1. Energies (Ryd) and lifetimes of the excitation levels.

Index	State	Level	Experiment	BSR	Difference	τ(ns)
1	$3p^6$	$^1S_0$	0.00000	0.00000	0.00000	
2	$3p^54s$	$^3P^o_2$	1.48083	1.48095	0.00012	
3		$^3P^o_1$	1.48748	1.48670	–0.00078	6.23
4	$3p^53d$	$^3P^o_0$	1.48930	1.48908	–0.00022	
5		$^3P^o_1$	1.49896	1.50041	0.00145	2.41
6		$^3P^o_2$	1.50293	1.50312	0.00019	
7	$3p^54s$	$^3P^o_0$	1.50492	1.50535	0.00043	
8		$^1P^o_1$	1.51687	1.51642	–0.00045	0.47
9	$3p^53d$	$^3F^o_4$	1.54960	1.54972	0.00012	
10		$^3F^o_3$	1.55673	1.55676	0.00003	
11		$^3F^o_2$	1.56303	1.56297	–0.00006	
12		$^1D^o_2$	1.63435	1.64301	0.00866	
13		$^3D^o_3$	1.63478	1.64395	0.00917	
14		$^3D^o_2$	1.64385	1.65273	0.00888	
15		$^3D^o_1$	1.64437	1.65357	0.00920	69.4
16		$^1F^o_3$	1.64592	1.65461	0.00869	
17	$3p^54p$	$^3S_1$	1.66948	1.66949	0.00001	8.69
18		$^3D_3$	1.69845	1.69858	0.00013	6.95
19		$^3D_2$	1.70117	1.70122	0.00005	7.54
20		$^3D_1$	1.70887	1.70879	–0.00008	7.15
21		$^1D_2$	1.71455	1.71472	0.00017	7.49
22		$^1P_1$	1.72448	1.72465	0.00017	7.51
23		$^3P_2$	1.72829	1.72841	0.00012	6.47
24		$^3P_0$	1.72929	1.72936	0.00007	5.91
25		$^3P_1$	1.73260	1.73252	–0.00008	6.42
26		$^1S_0$	1.77490	1.78391	0.00901	3.93
27	$3p^53d$	$^1P^o_1$	1.84045	1.85249	0.01204	0.07
28	$3p^55s$	$^3P^o_2$	1.94090	1.94081	0.00009	4.15
29		$^3P^o_1$	1.95670	1.94423	0.01247	1.91
30		$^3P^o_0$	1.95936	1.95961	0.00025	4.09
31		$^1P^o_1$	1.96046	1.96179	0.00133	1.84
32	$3p^54d$	$^3P^o_0$	1.96288	1.96784	0.00496	2.90
33		$^3P^o_1$	1.96698	1.96870	0.00172	2.90
34		$^3P^o_2$	1.96825	1.97245	0.00420	3.02
35		$^3F^o_4$	1.97258	1.97693	0.00435	2.92
36		$^3F^o_3$	1.97801	1.98112	0.00311	2.95
37		$^3F^o_2$	1.98403	1.98526	0.00173	3.05
38		$^3D^o_3$	1.98412	1.99371	0.00959	3.25
39		$^1D^o_2$	1.99485	2.00055	0.00570	3.18
40		$^3D^o_1$	1.99574	2.00375	0.00801	2.50
41		$^3D^o_2$	1.99743	2.00530	0.00787	3.22
42		$^1F^o_3$	1.99897	2.00762	0.00865	3.19
43		$^1P^o_1$	2.06556	2.06616	0.00006	0.20

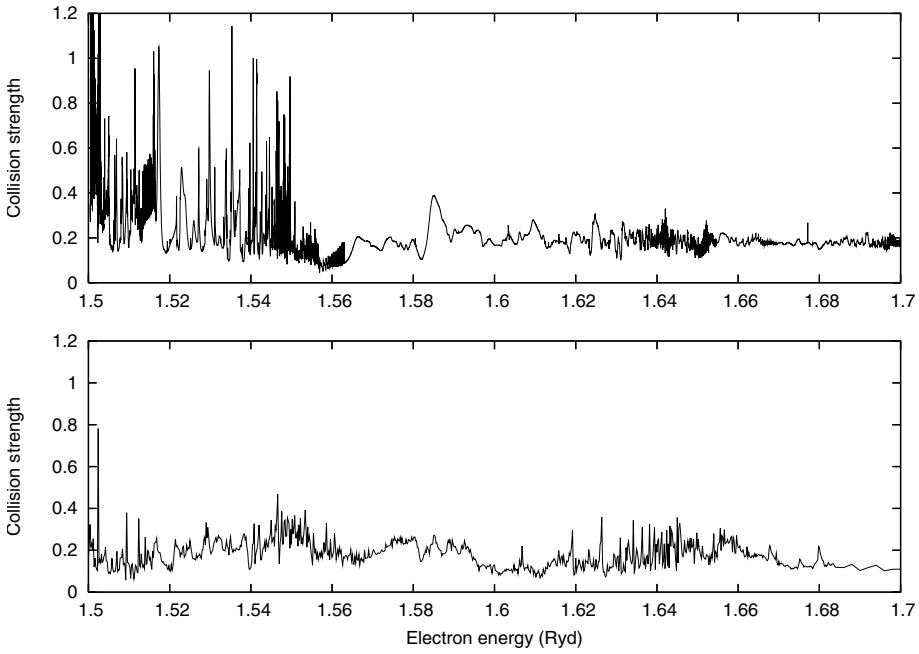

Fig. 1. Collision strengths for the intercombination $3p^6\ ^1S_0$–$3p^5 3d\ ^3P^o_1$ (1–5) transition as a function of electron energy between the $3p^5 3d\ ^3P^o_1$ and $3p^5 4p\ ^3D_2$ thresholds. Present results, upper panel; Berrington et al. (2006), lower panel.

accuracy criterion. There is normally a very good agreement between the present length and velocity forms of oscillator strengths.

3. Collision strengths

The scattering calculations were carried out with a new general R-matrix code (Zatsarinny 2006), in which non-orthogonal orbitals are used to describe both the target levels and the R-matrix continuum basis functions. In our work the scattering orbitals were constructed orthogonal to the 1s, 2s, 2p, 3s and 3p core orbitals and to the spectroscopic valence 4s, 3d, 4p, 5s and 4d orbitals. No orthogonality constraints to the correlated orbitals have been imposed. Thus the bound part of the close-coupling expansions contained only a limited number of configurations. We chose 87 continuum basis functions for each angular momentum and a R-matrix box of radius $a = 30$ au to contain all atomic orbitals. The relativistic effects in the scattering calculations have been incorporated in the Breit-Pauli Hamiltonian through the use of Darwin, mass correction and spin-orbit operators. The scattering parameters are then found by matching the inner solution at $r = a$ to the asymptotic solutions in the outer region. The calculations include all scattering symmetries with $J \leq 50.5$ and these are estimated to give converged results for many forbidden transitions. The higher partial waves contributions ($J \geq 51.5$) for the dipole-allowed transitions are calculated using the Coulomb-Bethe approach and a top-up procedure based on geometric series approximation for the non-allowed transitions.

We chose a fine-energy grid of 10^{-5} Ryd in the closed-channel energy region up to 2.1 Ryd. This allowed us to delineate important resonance structures almost completely in the collision strengths. At higher energies where all channels are open and there are no resonances, the collision strengths show smooth behavior and we use an energy grid of 0.1 Ryd. The collision strength calculations are performed in the energy range from threshold to 30.0 Ryd. The collision strengths for the intercombination $3p^6\ ^1S_0$–$3p^5 3d\ ^3P^o_1$ (1–5) and forbidden $3p^6\ ^1S_0$–$3p^5 4p\ ^3S_1$ (1–17) and $3p^6\ ^1S_0$–$3p^5 4p\ ^3D_2$ (1–19) transitions have been displayed as a function of incident electron energy from $3p^5 3d\ ^3P^o_1$ threshold to the $3p^5 4p\ ^3D_2$ threshold at 1.7 Ryd in Fig. 1 and from threshold to $3p^5 4d\ ^1P^o_1$ threshold around 2.0 Ryd in Figs. 2 and 3. Our results (upper panel) have been compared with the calculation of Berrington et al. (2006) (lower panel). The resonance structures are almost completely resolved with a very fine energy mesh in our calculation, whereas Berrington et al. (2006) appear to use a coarse energy mesh. The resonance structures are very complex and quite dense due to many overlapping Rydberg series converging to various thresholds. The background collision strengths away from resonances appear to be very similar from the two calculations, but there are differences in magnitude and position of resonances. The differences are mostly caused by the wave functions used in target descriptions and by the scattering models. The resonances make substantial enhancements in collision strengths for many transitions. Our calculation adequately account for the short-range electron correlation to ensure correct position of resonances in the low energy region.

We have displayed collision strengths for the $3p^6\ ^1S_0$–$3p^5 3d\ ^3P^o_1$ (1–5) (upper curves), $3p^6\ ^1S_0$–$3p^5 4p\ ^3S_1$ (1–17) (lower curves) and $3p^6\ ^1S_0$–$3p^5 4p\ ^3D_2$ (1–19) (middle curves) transitions in the energy region from 2.5 to 30.0 Ryd in Fig. 4 where all channels are open and collision strengths are expected to show smooth variation. Our results are compared with the calculation of Berrington et al. (2006). There is a reasonable agreement between the two calculations, particularly for the weaker forbidden $3p^6\ ^1S_0$–$3p^5 4p\ ^3S_1$ (1–17) and $3p^6\ ^1S_0$–$3p^5 4p\ ^3D_2$ (1–19) transitions. It may be noted that our collision strengths show a smooth behavior with energy, but the results of Berrington et al. (2006) contain pseudoresonance structures in the energy region up to about 14.0 Ryd. Our results for the $3p^6\ ^1S_0$–$3p^5 3d\ ^3P^o_1$ (1–5) transition are higher than the calculation of Berrington et al. (2006) by 10% to 16% at incident electron energies above 14.0 Ryd. The discrepancies between the two calculations for the $3p^6\ ^1S_0$–$3p^5 3d\ ^3P^o_1$ (1–5) transition perhaps have been caused by the differences in target wave functions, scattering models and the number of partial waves. The inclusion of pseudostates and additional ($N + 1$) terms in the calculation of Berrington et al. (2006) may account for coupling to higher autoionizing and continuum levels and thus reduce the collision strength

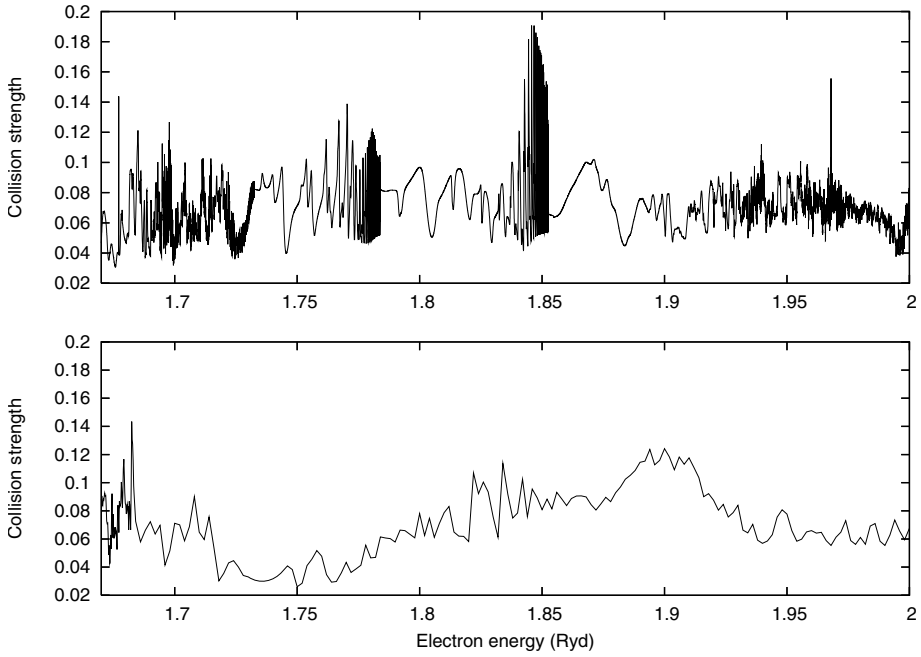

Fig. 2. Collision strengths for the forbidden $3p^6\ {}^1S_0$–$3p^5 4p\ {}^3S_1$ (1–17) transition as a function of electron energy between the $3p^5 4p\ {}^3S_1$ and $3p^5 4d\ {}^1P^o_1$ thresholds. Present results, *upper panel*; Berrington et al. (2006), *lower panel*.

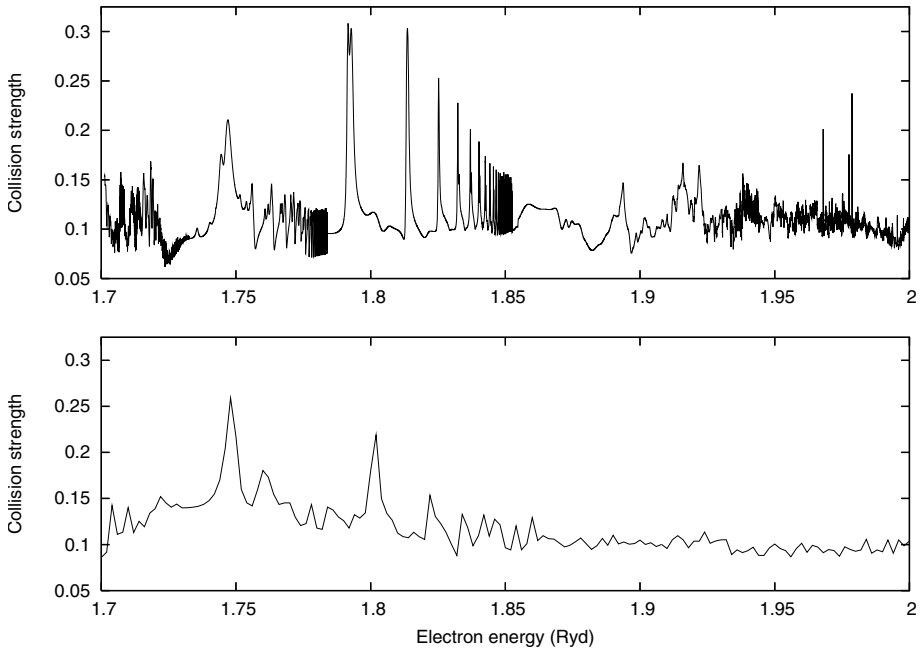

Fig. 3. Collision strengths for the forbidden $3p^6\ {}^1S_0$–$3p^5 4p\ {}^3D_2$ (1–19) transition as a function of electron energy between the $3p^5 4p\ {}^3D_2$ and $3p^5 4d\ {}^1P^o_1$ thresholds. Present results, *upper panel*; Berrington et al. (2006), *lower panel*.

at intermediate energies. The cause of differences for 1–27 transition appears to be the same. It may be noted that Berrington et al. (2006) included up to $J = 14.5$ partial waves and applied a top-up. The non-resonant background collision strengths for the allowed transitions are normally larger than for the forbidden and intercombination transitions, while the resonance enhancement in collision strengths for the forbidden and intercombination transitions are generally larger compared to allowed transitions. We present collision strengths for all transitions between the 43 levels at seven incident electron energies 2.1, 4.0, 6.0, 8.0, 12.0, 16.0 and 20.0 Ryd in Table 3. The indices of initial and final levels of a transition (i–j) are given in the first column of Table 3 and these are taken from Table 1. These energies are above the highest excitation threshold at 2.066 Ryd where collision strength varies smoothly with incident electron energies. The collision strengths for different types of transitions generally show expected energy behavior in the higher energy region. The collision strengths for dipole-allowed transitions exhibit logarithmic behavior whereas collision strengths for intercombination transitions fall-off rapidly with increasing energy.

4. Effective collision strengths

We have calculated effective collision strengths by integrating the collision strengths over a Maxwellian distribution of electron energies. We have presented effective collision strengths for all transitions between the lowest 43 fine-structure levels considered in our work in Table 4. The indices of lower and upper levels of a transition are given in Table 1. The results are presented at 11 temperatures in the range $\mathrm{Log}_{10}\ T = 3.3$–$5.6$ K suitable for modeling of astrophysical plasmas. The results for transitions to higher excitation levels may be somewhat uncertain because of the neglect of coupling with exciting levels above level 43. The effective collision strength for the allowed transitions increases

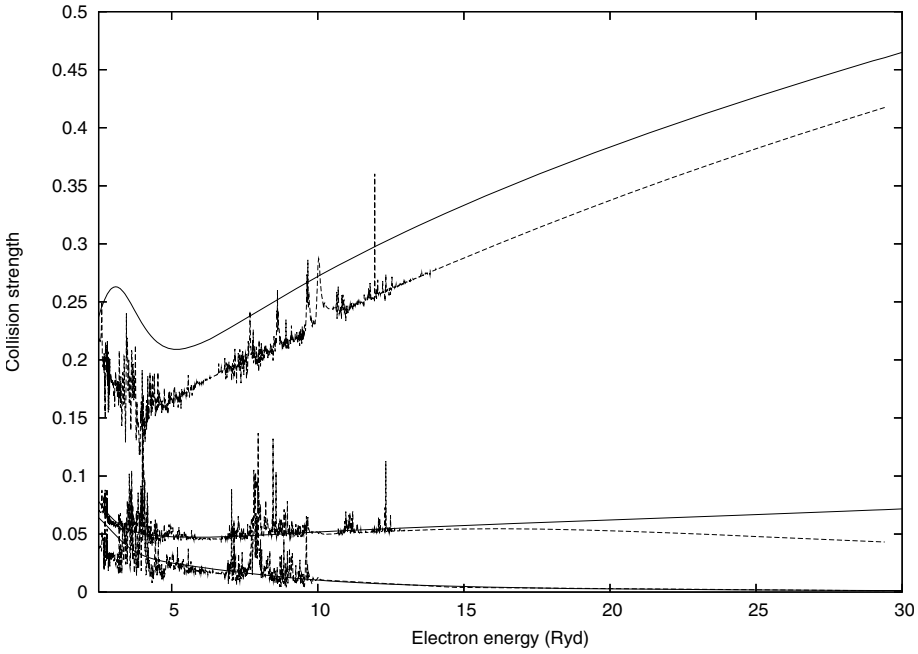

Fig. 4. Collision strengths for the $3p^6\ {}^1S_0$–$3p^5 3d\ {}^3P^o_1$ (1–5) (*upper curves*), $3p^6\ {}^1S_0$–$3p^5 4p\ {}^3S_1$ (1–17) (*lower curves*) and $3p^6\ {}^1S_0$–$3p^5 4p\ {}^3D_2$ (1–19) (*middle curves*) transitions as a function of electron energy in all open channels region. Present results, solid curve; Berrington et al. (2006), dashed curve.

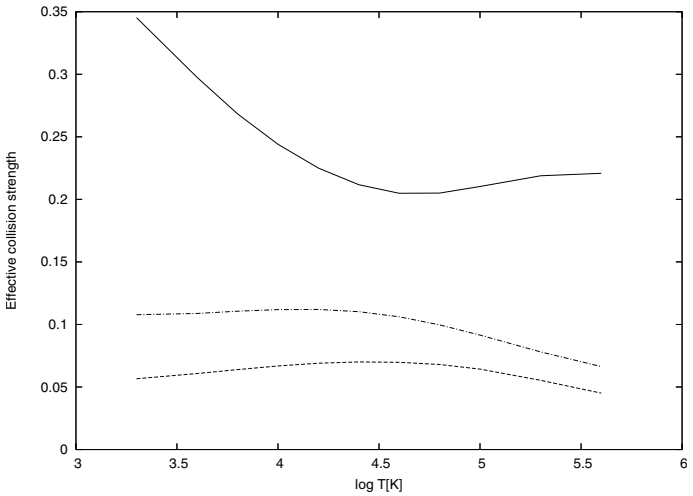

Fig. 5. Effective collision strengths for the $3p^6\ {}^1S_0$–$3p^5 3d\ {}^3P^o_1$ (1–5) (solid curve), $3p^6\ {}^1S_0$–$3p^5 4p\ {}^3S_1$ (1–17) (dashed curve) and $3p^6\ {}^1S_0$–$3p^5 4p\ {}^3D_2$ (1–19) (dash-dotted curve) transitions as a function of electron temperature.

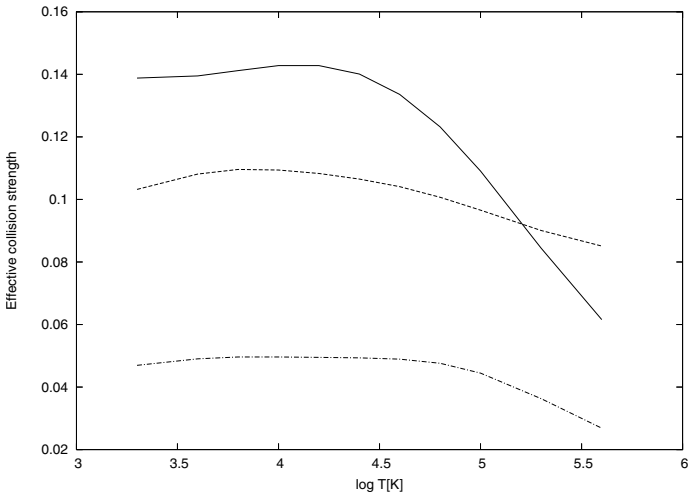

Fig. 6. Effective collision strengths for the forbidden $3p^6\ {}^1S_0$–$3p^5 4p\ {}^3D_3$ (1–18) (solid curve), $3p^6\ {}^1S_0$–$3p^5 4p\ {}^1D_2$ (1–21) (dashed curve) and $3p^6\ {}^1S_0$–$3p^5 4p\ {}^3P_1$ (1–25) (dash-dotted curve) transitions as a function of electron temperature.

with increasing temperature and the effective collision strength for the intercombination transitions decreases with increasing temperature in the high-temperature regime. The intercombination transitions can occur only through electron exchange.

We have plotted effective collision strengths for the $3p^6\ {}^1S_0$–$3p^5 3d\ {}^3P^o_1$ (1–5), $3p^6\ {}^1S_0$–$3p^5 4p\ {}^3S_1$ (1–17) and $3p^6\ {}^1S_0$–$3p^5 4p\ {}^3D_2$ (1–19) transitions as a function of electron temperature in the range $\mathrm{Log}_{10}\ T = 3.3$–$5.6$ K in Fig. 5. To the best of our knowledge there are no other previous effective collision strengths available to compare with our results. The high quality wave functions that take adequate account of the term dependence of valence orbitals and of relaxation effects have been used in our calculation. However, we have not checked on the coupling effects from higher lying excitation levels. The effective collision strengths for the forbidden $3p^6\ {}^1S_0$–$3p^5 4p\ {}^3D_3$ (1–18), $3p^6\ {}^1S_0$–$3p^5 4p\ {}^1D_2$ (1–21) and $3p^6\ {}^1S_0$–$3p^5 4p\ {}^3P_1$ (1–25) transitions are shown in Fig. 6 as a function of electron temperature. The effective collision strengths for the forbidden transitions generally display a slow fall-off with increasing temperature. The effective collision strengths for the forbidden $3p^6\ {}^1S_0$–$3p^5 4p\ {}^3D_3$ (1–18) transition decrease more rapidly than for the $3p^6\ {}^1S_0$–$3p^5 4p\ {}^1D_2$ (1–21) and $3p^6\ {}^1S_0$–$3p^5 4p\ {}^3P_1$ (1–25) transitions.

5. Discussion and conclusions

There are generally two major sources of error in any close-coupling scattering calculation: target description and convergence of close-coupling expansion. Based on a comparison of calculated excitation energies and oscillator strengths with experiments and other reliable calculations as well as the fact that we used a well tested sound approach, our wave functions appear to be of high quality to yield an accurate target description. The excitation energies of the target levels shown in Table 1

demonstrate that our theory deviates from experiment by less than 0.5% for all but 7 excited levels (12–16, 26 and 29) where the percentage deviation is generally less than 0.6%. The worst agreement is for the $3p^5 3d\ ^1P^o_1$ level which deviates from the experiment by 0.65%. The excitation energies depend to first order on the accuracy of wave functions, while oscillator strengths depend to second order and thus can provide a better test of the wave functions. A detailed comparison of oscillator strengths from the ground $3p^6\ ^1S_0$ and first metastable $3p^5 4s\ ^3P^o_2$ levels with other calculations and experiment was presented by Tayal & Zatsarinny (2008) who noted a reasonable agreement with other reliable calculations. Our radiative parameters are estimated to be accurate to about 5%.

A sufficient number of target states in the close-coupling expansion are required to achieve convergence for the transitions of interest. This factor may introduce varied amount of uncertainties in different transitions. The collision strengths for transitions between the levels of $3p^6$, $3p^5 4s$, $3p^5 3d$ and $3p^5 4p$ configurations are well converged in our calculation. The transitions from the ground $3p^6\ ^1S_0$ level to the $3p^5 4s$, $3p^5 3d$ and $3p^5 4p$ levels should be most accurate (∼15%) and somewhat less accurate (∼20%) for transitions between excited levels. For higher levels of the $3p^5 4d$ configuration there may be significant coupling effects from higher autoionizing and continuum states and thus our results for transitions involving $3p^5 4d$ levels may be less accurate (∼25% or worse). It may also be noted that we used a very fine-energy mesh (10^{-5} Ryd) in the threshold energy region to resolve almost all resonances and performed scattering calculation up to 30.0 Ryd. The B-spline R-matrix calculations were carried out for partial waves up to $J = 50.5$. The top-up procedures based on the Coulomb-Bethe approach for the allowed transitions and geometric progression approach for non-allowed transitions were used to estimate the contributions for $J \geq 51.5$. These scattering parameters were considered sufficient and not to cause any further significant uncertainties in our results.

In conclusion, we have presented accurate oscillator strengths and effective collision strengths for K II lines among the 43 fine-structure levels. We used non-orthogonal orbitals for the construction of CI wave functions for target levels and for the representation of scattering functions. The checks on excitation energies and oscillator strengths provide us confidence that our target wave functions are likely to be accurate to yield reliable collision strengths from the B-spline Breit-Pauli R-matrix scattering calculations. The present target wave functions contain both the valence and core-valence correlation, together with the relaxation effects due to the strong penetration of the 3d electron in the core. We have attempted to account for important physical effects such as electron correlation, relativistic, and channel coupling effects. The Rydberg series of resonances converging to several excited levels are found to enhance collision strengths substantially. The effective collision strengths are presented over a wide range of electron temperatures suitable for use in astrophysical plasmas modeling. We have also reported accurate radiative rates for E1 transitions using non-orthogonal wave functions in multiconfiguration Hartree-Fock approach which are of considerable interest in astrophysical applications.

Acknowledgements. This research work is supported by NASA grant NNX09AB63G from the Planetary Atmospheres program. The authors would like thank Professor K. A. Berrington for sending their collision strength data in electronic form.

References

Beck, D. R. 2002, J. Phys. B, 35, 4155
Berrington, K. A., Nakazaki, S., & Murakami, Y. 2006, J. Phys. B, 39, 4733
Fegley, B., & Zolotov, M. Y. 2000, Icarus, 148, 193
Froese Fischer, C. 1991, Comput. Phys. Commun., 64, 369
Henderson, M., Curtis, L. J., Matulioniene, R., Ellis, D. G., & Li, Y. 1997, Phys. Rev. A, 55, 2733
Kuppers, M., & Schneider, N. M. 2000, Geophys. Res. Lett., 27, 513
Peterson, K., Ekberg, J. O., Martinson, I., & Reader, J. 2007, Phys. Scr., 75, 702
Smirnov, Y. M., & Shapochkin, M. B. 1979, Opt. Spectrosc., 47, 6
Tayal, S. S., & Zatsarinny, O. 2008, Phys. Rev. A, 78, 012713
Zapesochny, A. I., Imre, A. I., Aleksakhin, I. S., Zapesochny, I. P., & Zatsarinny, O. I. 1986, Sov. Phys. JETP, 63, 1155
Zatsarinny, O. 2006, Comput. Phys. Commun., 124, 247
Zatsarinny, O., & Froese Fischer, C. 2000, Comput. Phys. Commun., 124, 247